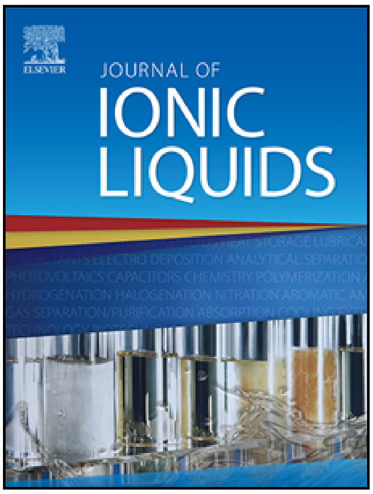

Expanding chemical space of ionic liquid based aqueous biphasic systems with thiocyanate

Gabriel L. Camilo , Murilo L. Alcantara , Ana M. Ferreira ,
Marco Prazeres , Catarina M.S.S. Neves , João A.P. Coutinho

PII: S2772-4220(26)00024-8
DOI: https://doi.org/10.1016/j.jil.2026.100210
Reference: JIL 100210

To appear in: *Journal of Ionic Liquids*

Received date: 12 February 2026
Revised date: 28 April 2026
Accepted date: 6 May 2026

Please cite this article as: Gabriel L. Camilo , Murilo L. Alcantara , Ana M. Ferreira , Marco Prazeres , Catarina M.S.S. Neves , João A.P. Coutinho , Expanding chemical space of ionic liquid based aqueous biphasic systems with thiocyanate, *Journal of Ionic Liquids* (2026), doi: https://doi.org/10.1016/j.jil.2026.100210

Expanding chemical space of ionic liquid based aqueous biphasic systems with thiocyanate

Gabriel L. Camilo[1], Murilo L. Alcantara*[1], Ana M. Ferreira[1], Marco Prazeres[1], Catarina M.S.S. Neves[1], João A. P. Coutinho*[1]

[1]*CICECO - Aveiro Institute of Materials, University of Aveiro, Campus Universitário de Santiago, 3810-193 Aveiro, Portugal.*

*Corresponding authors:

murilo.la@ua.pt

jcoutinho@ua.pt

Abstract

Membrane-free redox flow batteries (RFBs) offer a cost-effective alternative to conventional systems by eliminating ion-selective membranes, thereby reducing both capital costs and ohmic resistance. These systems require careful selection of electrolyte components and redox-active organic molecules (ROMs) to ensure efficient electrolytes with limited cross-contamination. This study evaluated the use of sodium thiocyanate (NaSCN) as an additive to expand the chemical space of ionic-liquid-based electrolytes, and reduce cross-contamination of ROMs. It was found that NaSCN promotes liquid-liquid phase separation in systems that otherwise present only solid-liquid equilibria, which are unsuitable for RFB applications. Partition coefficients of six promising organic and inorganic redox-active compounds were measured, revealing formulation-dependent trends that vary with ionic-liquid family, hydrophilicity and NaSCN content. Partial replacement of the ionic liquid with NaSCN reduces the estimated material cost of the electrolyte by 21-24% without compromising partitioning, thereby addressing both cost and cross-contamination challenges.

Keywords: Aqueous biphasic systems, Ionic liquid, Sodium thiocyanate, redox-active molecules, Partition coefficients, Membrane-free redox flow batteries

1 Introduction

Energy storage systems (ESSs) have evolved from simple storage units into key components of modern power systems, providing high power and energy density, rapid response, reliable energy supply, and enhanced system security, a transition supported by advances in power electronics and electricity market developments [1,2]. At the same time, climate change and the well-established link between greenhouse gas emissions and fossil fuel-based power generation have intensified the global shift toward renewable energy sources. However, the intermittent nature of renewable energy supply often leads to a mismatch between generation and demand, requiring backup power to ensure grid reliability [3,4]. As renewable penetration increases and global energy demand continues to grow, the deployment of additional energy storage systems (ESSs) becomes essential to balance supply and demand, reduce reliance on backup plants, and enable significant reductions in greenhouse gas emissions [5,6].

Within electrochemical ESSs, redox flow batteries (RFBs) are promising technologies for large-scale sustainable energy storage and stand out for large-scale stationary applications due to their decoupled power and energy, long cycle life, and flexible design [7,8]. However, conventional RFBs rely on costly ion-exchange membranes to keep redox-active species separated while allowing the transport of small ions for charge balance [9,10]. Strategies based on electrolyte and molecular design have been explored to mitigate crossover and performance losses, taking advantage of the high tunability of redox-active species to improve solubility, stability, electrochemical kinetics, and operating voltage windows [11,12]. Building on these advances, membrane-free RFB concepts have emerged as an alternative approach in which crossover control is achieved through electrolyte phase separation rather than ion-exchange membranes [13,14].

Membrane-free redox flow batteries rely on biphasic electrolytes that confine redox-active organic molecules (ROMs) [15,16], or other redox-active compounds, in distinct liquid phases, eliminating ion-exchange membranes and mitigating crossover contamination and ROM losses [17,18]. Rather than opposing thermodynamic mixing, the membrane-free concept leverages it. By employing immiscible electrolytes that promote strong partitioning of redox-active species, membrane-free RFBs can operate without physical separators, potentially reducing ohmic resistance [19,20]. This motivation is also economic: ion-selective membranes are a major cost driver in conventional RFB stacks (often discussed as ~30% of total system cost), so a viable membrane-free electrolyte must justify any added formulation complexity or additives used to enforce phase separation [17,21].

Stable membrane-free RFB operation has already been demonstrated [22] and patented [23]. Nevertheless, achieving sufficiently low crossover remains a critical prerequisite for ensuring efficient and durable RFB operation [17,19]. In this scenario, ionic-liquid-based aqueous biphasic systems (ABS) are attractive candidates because they combine high ionic conductivity, broad chemical tunability and low interfacial resistance [24,25].

However, their applicability remains constrained by two major limitations: (i) many hydrophilic ionic liquids (ILs) combined with conventional salting-out agents such as ammonium sulfate ($(NH_4)_2SO_4$) form only solid-liquid equilibria instead of true liquid-liquid equilibria [14]; and (ii) only a narrow subset of ROMs exhibits adequate partitioning in currently available formulations [17,18]. These constraints restrict the accessible design space for membrane-free RFBs.

Designing selective and stable ABS for energy storage requires precise control over the interactions that govern phase separation and solute distribution. Anion identity strongly affects phase behavior and ROM partitioning in IL-based ABS [26]. These observations suggest that anion effects may be a strategic approach for tuning both biphasic behavior and ROM selectivity [27].

This concept has recently gained attention in membrane-free RFB electrolyte design. A recent study [24] demonstrated that NaSCN addition can modulate ROM partitioning in IL-based ABS that already exhibit liquid-liquid separation, highlighting sodium thiocyanate as a promising additive for increasing ROM partitioning on IL-based ABS, and reducing cross-contamination on membrane-free RFBs. This effect is attributed to the high aqueous solubility and electrochemical compatibility of Na^+, together with the weak hydration and high polarizability of SCN^- [28,29]. This behavior is consistent with the strongly chaotropic nature of SCN^- in the Hofmeister series, characterized by low hydration free energy and a strong capacity to disrupt water structure and ion-water interactions, in contrast to more strongly hydrated anions such as Cl^- and SO_4^{2-} [30]. However, existing studies have largely focused on systems that are already biphasic, overlooking the potential of additives such as NaSCN to induce liquid-liquid phase separation in systems that remain monophasic or form solid-liquid equilibria.

In this context, this study investigates whether NaSCN can induce liquid-liquid phase separation in chloride-based IL + ammonium sulfate + water systems that do not exhibit biphasic behavior under conventional conditions. The partitioning of representative redox-active species was evaluated to identify promising systems for membrane-free redox flow battery applications, and a cost assessment was performed to quantify the impact of partial IL substitution with NaSCN. By combining phase behavior, partitioning data, and cost considerations across different IL families, this work establishes a systematic screening framework for expanding the accessible electrolyte design space and identifies NaSCN as a practical additive for enabling and tuning biphasic behavior in membrane-free redox flow batteries.

2 Materials and methods

2.1 Materials selection

The ionic liquids were selected to cover a range of cationic structures and hydrophobicity in order to evaluate the influence of molecular architecture on phase behavior. The chloride ionic liquids (IL-Cl) studied were $[C_2mim]Cl$, $[C_4mim]Cl$, $[C_4mpyr]Cl$, $[C_4mpip]Cl$, $[C_4mpy]Cl$, $[N_{2222}]Cl$, and $[N_{3333}]Cl$. These ILs include aromatic (imidazolium [im] and pyridinium [py]), cyclic aliphatic (pyrrolidinium [pyr] and piperidinium [pip]), and linear aliphatic (tetraalkylammonium $[N_{xxxx}]$) cations. Chloride ILs were selected for this study for presenting high hydrophilicity and capacity to form ABS with proven applicability as electrolytes on membrane-free RFB [14]. The selected IL-Cl systems differ in alkyl-chain length, ring size, and hydrophobicity, allowing comparison of structural effects on ABS phase behavior. Ammonium sulfate ($(NH_4)_2SO_4$) was used as salting-out agent due to its strong kosmotropic character and its well-established ability to induce phase separation in IL-based ABS [14].

The redox-active molecules (ROMs) used were chosen for presenting promising reversible redox activity on aqueous electrolytes [14,24]. Methyl viologen (MV), benzyl viologen (BV), 2,2,6,6-Tetramethylpiperidine 1-oxyl (TEMPO), and 2,2,6,6-Tetramethyl-4-[1-oxo-6-(triethylammonio)hexylamino]-1-piperidinyloxy bromide (WS-TEMPO) differ in polarity, aqueous solubility, and are widely used as reference ROMs [31,32]. The use of these compounds extends the polarity range previously investigated in IL-based ABS and allows evaluation of the effect of NaSCN addition on ROM phase partitioning.

Potassium ferricyanide ($K_3[Fe(CN)_6]$) and potassium ferrocyanide ($K_4[Fe(CN)_6]$) were used as a classical inorganic redox pair. These species show high chemical stability and are widely used in aqueous redox systems. $K_4[Fe(CN)_6]$ has previously been explored in related membrane-free configurations [33]. The use of both oxidation states allows assessment of whether closely related species remain in the same phase in a membrane-free configuration. Overall, the selected organic and inorganic redox-active species provide a set of solutes with different charge, polarity, and redox properties for partitioning studies in IL-based ABS.

All materials used in this study are listed in Table 1, and their chemical structures are shown in Figure 1. All compounds were used as received without further purification.

Table 1. Name, acronym, purity and supplier of the ionic liquids, inorganic salts and redox species used in this work.

Name	**Acronym**	**CAS**	**Purity**	**Supplier**
1-Ethyl-3-methylimidazolium chloride	$[C_2mim]Cl$	65039-09-0	98.0 %	Iolitec
1-Butyl-3-methylimidazolium chloride	$[C_4mim]Cl$	79917-90-1	99.0 %	Iolitec
1-Butyl-1-methylpyrrolidinium chloride	$[C_4mpyr]Cl$	479500-35-1	99.0 %	Iolitec
1-Butyl-1-methylpiperidinium chloride	$[C_4mpip]Cl$	845790-13-8	99.0 %	Iolitec
1-Butyl-3-methylpyridinium chloride	$[C_4mpy]Cl$	125652-55-3	98.0 %	Iolitec
Tetraethylammonium chloride	$[N_{2222}]Cl$	56-34-8	98.0 %	Sigma
Tetrapropylammonium chloride	$[N_{3333}]Cl$	5810-42-4	98.0 %	Alfa Aesar
Sodium thiocyanate	NaSCN	540-72-7	98.0 %	Merck
Ammonium sulfate	$(NH_4)_2SO_4$	7783-20-2	99.5 %	Panreac
Methyl Viologen Dichloride Hydrate	MV	75365-73-0	98.0 %	Sigma
Benzyl Viologen Dichloride	BV	1102-19-8	97.0 %	Sigma
2,2,6,6-tetramethylpiperidine-1-oxyl radical	TEMPO	2564-83-2	98.0 %	Sigma
2,2,6,6-Tetramethyl-4-[1-oxo-6-(triethylammonio)hexylamino]-1-piperidinyloxy bromide	WS-TEMPO	762245-84-1	95.0 %	Sigma
Potassium hexacyanoferrate(III)	$K_3[Fe(CN)_6]$	13746-66-2	99.0 %	Panreac
Potassium hexacyanoferrate(II) trihydrate	$K_4[Fe(CN)_6]$	14459-95-1	99.5 %	Sigma

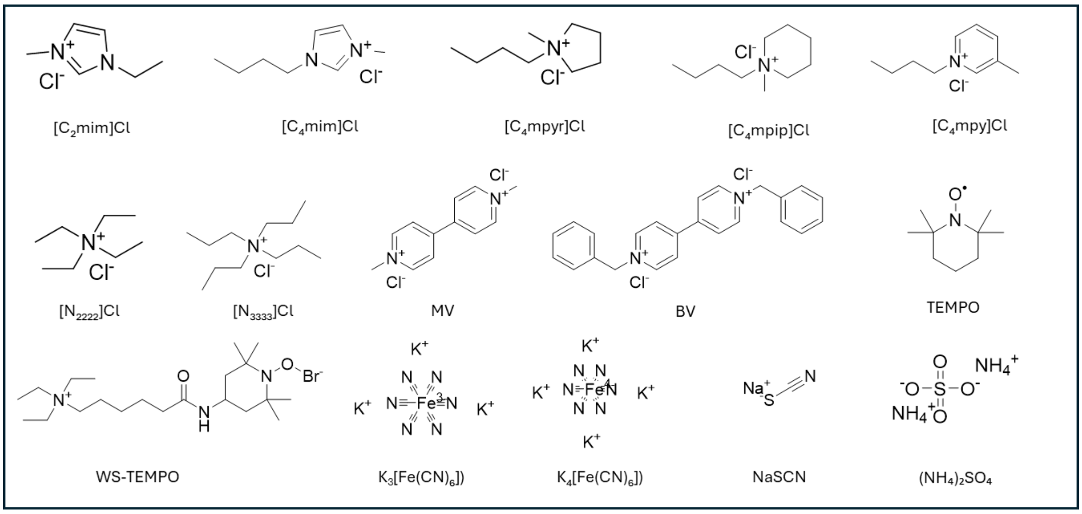

Figure 1. Chemical structures of the compounds used.

2.2 Aqueous biphasic systems

For the construction of the binodal curves, IL-Cl solutions were first converted in situ to IL-SCN by preparing IL-Cl + NaSCN mixtures at a 1:2 molar ratio. The binodal curves were then determined gravimetrically ($\pm 10^{-4}$ g) using the cloud-point titration method at 298 ± 1 K and atmospheric pressure, following established procedures [34]. In brief, a concentrated $(NH_4)_2SO_4$ solution (~40 wt%) was added dropwise to the homogeneous IL + NaSCN solution (~80 wt%) under continuous stirring until turbidity was observed, indicating the onset of phase separation. Water was subsequently added dropwise until the system returned to a clear monophasic state. This titration cycle was repeated to determine multiple binodal points. The mass of each component was recorded after each addition, and the binodal compositions were calculated by mass balance and expressed as mass fractions of IL (or IL-Cl + NaSCN), $(NH_4)_2SO_4$, and water.

For systems containing NaSCN, the salt was introduced by partially replacing the ionic liquid at a fixed IL:NaSCN molar ratio of 1:2. This ratio was selected to promote extensive anion exchange ($Cl^- \rightarrow SCN^-$) and ensure that phase behavior reflects SCN^--rich conditions rather than mixed Cl^-/SCN^- environments. Ion chromatography results reported in the literature show that even a 1:1 NaSCN:IL ratio leads to near-complete exchange [24]. The 1:2 ratio therefore minimizes residual chloride effects across all studied systems. The use of a fixed ratio also ensures consistent comparison across different ionic liquids and that the observed phase separation is primarily governed by SCN^-.

2.3 Partition coefficients of redox-active species

The partitioning of MV, BV, TEMPO, WS-TEMPO, $K_3[Fe(CN)_6]$, and $K_4[Fe(CN)_6]$ was quantified using a UV-Vis microplate reader (BioTek, Synergy HT). The selected wavelengths were 257 nm for MV and BV, 270 nm for TEMPO and WS-TEMPO, and 300 nm for $K_3[Fe(CN)_6]$ and $K_4[Fe(CN)_6]$.

ABS containing the redox species were prepared at compositions located well within the biphasic region, using IL systems with IL:NaSCN molar ratios of 1:2 (reference condition, according to the binodal curve) and 1:1 to evaluate the effect of NaSCN concentration. The specific compositions of all mixture points, expressed in mass fractions, are provided in the Supplementary Material (Tables S1 to S3). The systems were allowed to equilibrate overnight at ambient temperature and pressure. After equilibration, the IL-rich (top) and salt-rich (bottom) phases were carefully separated and analyzed by UV-Vis spectrophotometry.

The partition coefficient (*K*) was calculated as the ratio between the redox species concentration in the IL-rich phase (top) and salt-rich phase (bottom) ($K = [C]_{Top}/[C]_{Bottom}$). Three independent extraction experiments were performed to obtain mean values and corresponding standard deviations.

2.4 Cost estimation

Cost estimations were performed for the materials required to prepare ABS at the laboratory scale for membrane-free RFB applications. Two IL:NaSCN molar ratios (1:1 and 1:2) were compared using the experimentally studied ABS compositions. Relative changes were calculated based on $|K|$. Cost estimates correspond to the total ABS formulation (€/kg) and were derived from commercial laboratory-scale prices, serving exclusively for relative comparison between systems. Additional information is provided in the Supplementary Material (Table S4), including reagent prices, masses, and purities.

3 Results and discussion

3.1 Phase Equilibria and Biphasic Behavior

Exploratory evaluations of ABS formation were performed by mixing IL aqueous solutions (~80 wt%) with ammonium sulfate solutions (~40 wt%). The purpose was to evaluate if solid-free liquid-liquid biphasic systems could be formed with the studied ILs without the addition of NaSCN.

Solid precipitation was observed in all experiments, with no liquid-liquid regime identified, regardless of the IL used ([C_2mim]Cl, [C_4mim]Cl, [C_4mpyr]Cl, [C_4mpip]Cl, [C_4mpy]Cl, [N_{2222}]Cl). The only exception was the [N_{3333}]Cl, whose mixture with ammonium sulfate formed a clear liquid-liquid biphasic system. This exception highlights the strong influence of cation size on the solid precipitation, since [N_{2222}]Cl promotes solid precipitation while [N_{3333}]Cl and [N_{4444}]Cl can produce a liquid-liquid region (as also confirmed by the literature [14,24]).

Although the precipitated solid was not directly characterized, literature reports for similar IL + inorganic salt + water systems indicate that solid formation under strong salting-out conditions is typically associated with the inorganic salt, resulting from competition between the ionic liquid and the salting-out agent for hydration water. Under these conditions, the system may evolve toward a solid-liquid regime rather than liquid-liquid separation. Najdanovic-Visak et al. [35] reported that such systems may transition from liquid-liquid separation to inorganic salt precipitation as water availability falls below the solubility threshold of the inorganic salt.

The occurrence of solid precipitation in nearly all experiments highlights the restriction that solid-liquid equilibria impose on the range of IL compositions accessible for ABS formation. By replacing part of the IL with NaSCN at an IL:NaSCN molar ratio of 1:2, solid-free liquid-liquid systems could be formed with all chloride ILs that previously presented only solid-liquid equilibrium ([C_2mim]Cl, [C_4mim]Cl, [C_4mpyr]Cl, [C_4mpip]Cl, [C_4mpy]Cl, [N_{2222}]Cl).

A previous study using ion chromatography reported that the addition of NaSCN to chloride-based ionic liquids at an equimolar ratio (1:1, NaSCN:IL) promotes nearly complete anion exchange of Cl^- by SCN^- [24]. The NaSCN:IL molar ratio used in this work was 2:1, keeping NaSCN two times more concentrated than the chloride-based IL. Therefore, the IL chloride anions are expected to be largely exchanged by SCN^-. The Supplementary Material (Figure S1, Tables S5 to S8) compares phase transition curves of ILs containing SCN^- anions obtained either by direct synthesis or by mixing chloride-based ILs with NaSCN. The close agreement between these curves supports the occurrence of anion exchange.

Therefore, the introduction of the weakly hydrated thiocyanate anion was investigated as a strategy to promote liquid-liquid demixing in systems that remain monophasic or form solid-liquid equilibria in their chloride form. To obtain SCN^--enriched systems, each IL-Cl was combined with NaSCN at an IL:NaSCN molar ratio of 1:2, hereafter denoted as IL-Cl/SCN. Under these conditions, all IL-Cl/SCN systems exhibited liquid-liquid immiscibility, demonstrating that NaSCN addition and the resulting SCN^- enrichment effectively promote biphasic behavior for all ILs studied.

Figure 2 presents the liquid-liquid phase diagrams of these IL:NaSCN systems, which represent potential ABS candidates for membrane-free RFBs. The corresponding data are provided in the Supplementary Material (Tables S7-S13). The ability of the IL systems to promote liquid-liquid demixing follows the trend: $[N_{3333}]^+ > [C_4mpip]^+ > [C_4mpy]^+ > [C_4mpyr]^+ > [C_4mim]^+ > [N_{2222}]^+ > [C_2mim]^+$. This ranking broadly reflects increasing cation hydrophobicity, as more hydrophobic ionic liquids generally require lower IL contents to reach phase separation. Accordingly, increasing cation size and hydrophobicity shifts binodal curves to lower IL contents, in agreement with trends previously reported for ABS formation [27].

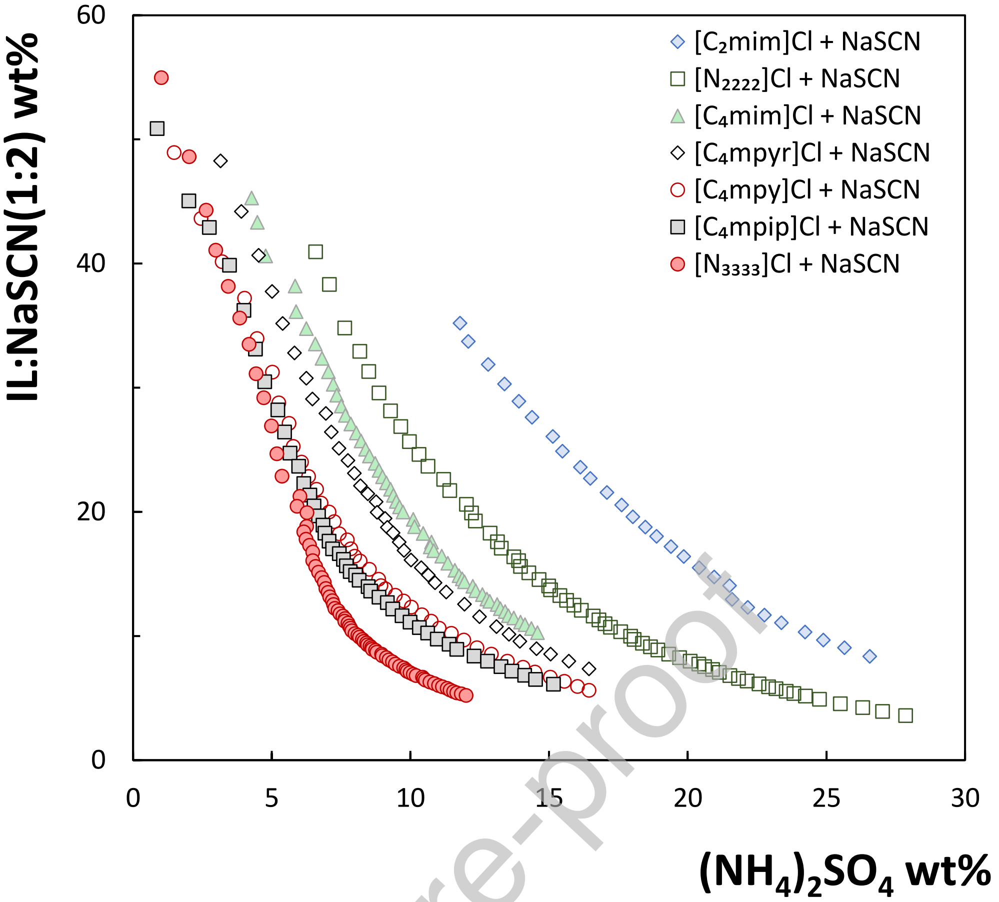

Figure 2. Binodal curves of ternary systems formed by ionic liquids, NaSCN and $(NH_4)_2SO_4$ at 298 K, expressed in mass fraction (wt%). Ionic liquids (IL) and NaSCN ratio are fixed at 1:2 molar ratio within composition range.

In this context, the weakly hydrated and highly polarizable SCN^- anion reduces the affinity of the IL-rich phase for water while strengthening salt-water interactions in the opposing phase, thereby increasing the polarity contrast between coexisting phases and promoting liquid-liquid separation [36]. Its Gibbs free energy of hydration (≈ −280 kJ mol^{-1}) is less negative than that of Cl^- (≈ −340 kJ mol^{-1}) and SO_4^{2-} (≈ −1080 kJ mol^{-1}) [37], reflecting weaker water binding and a greater tendency to disrupt hydration structures. These results indicate that SCN^- is a key factor enabling liquid-liquid phase separation in chloride-based ionic liquid systems, while the extent of the biphasic region remains strongly dependent on cation hydrophobicity.

3.2 Partition behavior of redox-active species

A feasible design of a membrane-free RFB requires not only the existence of biphasic electrolytes, but also the partition of suitable redox-active species to opposite phases. High partitions are required to reduce cross-contamination and self-discharge [10]. Four promising redox-active organic molecules (MV, BV, TEMPO, WS-TEMPO), and two inorganic ($K_3[Fe(CN)_6]$, and $K_4[Fe(CN)_6]$) were investigated in four chloride-based ionic liquids, namely $[C_2mim]Cl$, $[C_4mim]Cl$, $[N_{2222}]Cl$, and $[N_{3333}]Cl$. This selection enables assessment of the influence of cation family, aromaticity, and alkyl-chain length on solute distribution and on the effective polarity difference between the coexisting phases. All ABS were prepared with fixed amounts of ammonium sulfate and water, while the IL:NaSCN molar ratio varied from 1:1 to 1:2 to evaluate the effect of NaSCN concentration on redox-active species partitioning. Mixture points were selected within the biphasic region according to the binodal curves. The corresponding partition coefficients and mixture compositions are shown in Figure 3.

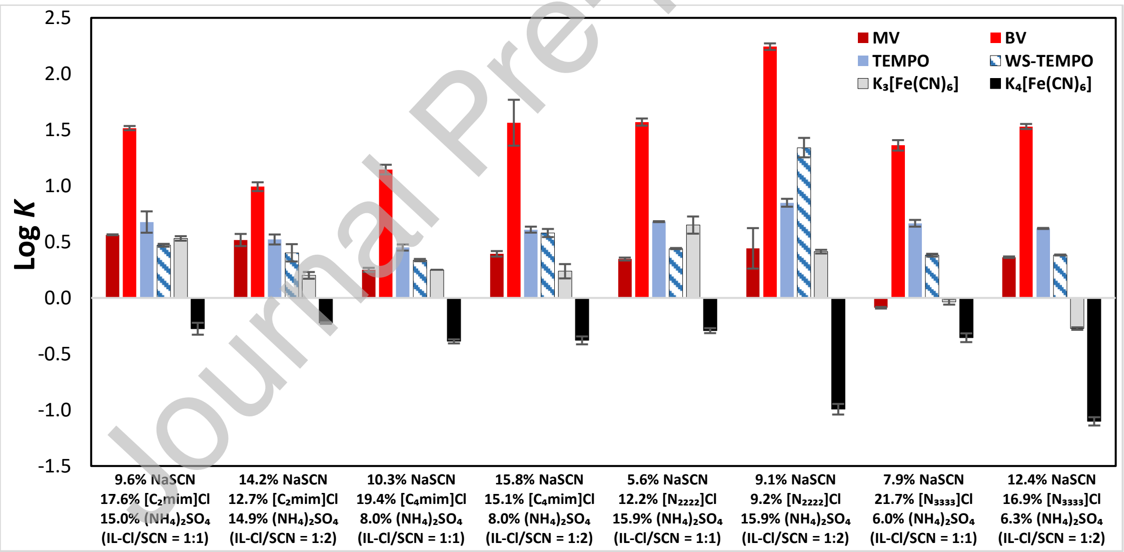

Figure 3. Partition behavior of redox-active compounds in IL-Cl/SCN aqueous biphasic systems at 298 K.

For ammonium-based ILs, particularly $[N_{2222}]Cl$, increasing NaSCN content led to a pronounced enhancement in the partitioning of most redox-active compounds, with the exception of $K_3[Fe(CN)_6]$. This behavior is consistent with previous observations showing that NaSCN addition and the resulting SCN^- enrichment of the IL-rich phase decrease its affinity for water, increasing the polarity difference between phases and enhancing solute partitioning [24]. Among the organic ROMs, benzyl viologen (BV) exhibited the most pronounced response to NaSCN addition, confirming its sensitivity to changes in phase differentiation.

The contrasting partitioning behavior of MV and BV highlights the role of molecular structure in determining phase preference. BV partitions strongly and consistently into the IL-rich phase across all investigated compositions. In contrast, MV exhibits composition-dependent behavior. In $[N_{2222}]$Cl-based systems, MV preferentially partitions into the IL-rich phase, whereas in $[N_{3333}]$Cl its partition coefficient is close to unity at low NaSCN contents and increases with NaSCN concentration, indicating a progressive shift in phase preference toward the IL-rich phase. Similar trends have been reported for $[N_{4444}]$Cl-based ABS in the absence of thiocyanate [24], underscoring the combined influence of cation size and hydrophobicity on solute distribution.

Across all systems, $K_4[Fe(CN)_6]$ consistently partitions into the hydrophilic, salt-rich phase, reflecting its strong hydration and ionic character. In contrast, $K_3[Fe(CN)_6]$ exhibits partial partition toward the IL-rich phase in systems formed with more hydrophilic ionic liquids, reflecting a reduced preference for the salt-rich phase relative to $K_4[Fe(CN)_6]$. Only $[N_{3333}]$Cl effectively confines both oxidation states of the ferrocyanide/ferricyanide couple to the hydrophilic phase (Figure 3), consistent with the larger polarity contrast achieved in ABS formed with more hydrophobic IL cations [36].

Imidazolium-based ILs exhibit a comparatively less pronounced change in partition values upon NaSCN addition. In $[C_4mim]$Cl, only modest changes in redox-active species partitioning are observed, while in $[C_2mim]$Cl higher NaSCN contents combined with lower IL concentrations lead to reduced partitioning. These trends reflect the stronger hydration and hydrogen-bonding capability of imidazolium cations, which limit the polarity contrast achievable between the coexisting phases, in agreement with previous studies on IL-based ABS [27]. These opposing trends reinforce that NaSCN substitution should be treated as a composition-level design variable rather than a universal performance enhancer, as further quantified in Table 2.

The distinct behavior between ammonium- and imidazolium-based ILs can be attributed to the role of the cation in governing phase formation and differentiation in ABS. Quaternary ammonium cations, due to their lower affinity for water, promote the formation of a less hydrated IL-rich phase, increasing the compositional contrast between the coexisting phases. In contrast, imidazolium cations exhibit stronger interactions with water, leading to more homogeneous systems and reduced phase separation. As a result, ammonium-based systems tend to form more clearly defined biphasic regions and exhibit enhanced phase differentiation, which contributes to improved partitioning of redox-active species [36].

TEMPO and WS-TEMPO display a strong and composition-independent preference for the IL-rich phase across all investigated systems, consistent with their neutral and hydrophobic character. In addition to phase selectivity, electrochemical compatibility between redox couples is essential for achieving high-voltage membrane-free RFBs. Because both TEMPO derivatives and the $K_3/K_4[Fe(CN)_6]$ redox couple exhibit relatively positive redox potentials [14], their co-partitioning into the same phase would be unfavorable for high-voltage membrane-free RFBs, as it would limit the accessible voltage window and increase the propensity for self-discharge. Consequently, although TEMPO-based redox couples show good solubility in the IL-rich phase, they are electrochemically incompatible with hydrophilic catholytes such as ferrocyanide in high-voltage membrane-free configurations.

The relevance of this partition-based screening for membrane-free RFBs is supported by previous studies demonstrating that IL-based ABS can operate as redox electrolytes in membrane-free configurations. Full-cell tests reported by Navalpotro et al. [14] using IL-ABS electrolytes containing MV and TEMPO demonstrated reversible cycling, selective partitioning of redox-active species, and cell voltages compatible with practical operation. In this context, although no full electrochemical validation is included in the present work, the partitioning and phase-behavior results reported here provide a reliable first screening step for identifying promising formulations for future membrane-free RFB studies.

Overall, quaternary ammonium-based ILs ($[N_{3333}]Cl$ and $[N_{2222}]Cl$) produced ABS with overall higher partitions compared to imidazolium-based ones. Regarding the partition of redox-active species, only potassium ferrocyanide ($K_4[Fe(CN)_6]$) showed consistent partitioning into the salt-rich bottom phase, especially in ABS formed with quaternary ammonium-based ILs. Therefore, only viologen/ferrocyanide combinations provide feasible catholyte/anolyte partition to opposite phases, on the studied ABS that could produce membrane-free RFB with low cross-contamination. Consequently, combinations of $K_3/K_4[Fe(CN)_6]$ with viologen derivatives such as MV or BV could potentially serve as redox pairs in the IL-based ABS under study.

3.3 Cost *vs.* Partition

The partial replacement of ionic liquids (ILs) with NaSCN in IL aqueous biphasic systems (ABS) was evaluated in terms of material cost and redox-active species partitioning performance.

Increasing the NaSCN content from an IL:NaSCN ratio of 1:1 to 1:2 resulted in a consistent reduction in formulation cost of 21-24% for all IL systems investigated (Table 2). This reduction originates from substituting a fraction of the IL, one of the most expensive electrolyte components [38], with NaSCN, a low-cost, abundant inorganic salt. Importantly, this cost benefit was largely independent of the IL cation, indicating that NaSCN substitution provides a robust and transferable economic advantage across different chemistries. The ionic liquid is the dominant cost contributor across all studied systems, while NaSCN and ammonium sulfate account for only a minor fraction of the total formulation cost, which explains why partial IL replacement drives the observed 21-24% cost reduction. It should be noted that catalogue prices may overestimate absolute costs relative to bulk industrial pricing, but relative cost ratios between systems remain informative for comparative screening purposes.

Table 2. Cost reduction and relative changes in redox-active species partitioning upon increasing the IL:NaSCN molar ratio from 1:1 to 1:2 in IL ABS.

		Partition increase % (1:1 → 1:2) *			
IL	**Cost Reduction % (1:1 → 1:2)**	**MV**	**BV**	**$K_3[Fe(CN)_6]$**	**$K_4[Fe(CN)_6]$**
[C$_2$mim]Cl	**24%**	-8%	-34%	-62%	-18%
[C$_4$mim]Cl	**21%**	57%	40%	-3%	-3%
[N$_{2222}$]Cl	**22%**	35%	43%	-37%	240%
[N$_{3333}$]Cl	**22%**	n/a†	12%	714%	211%

* Green shading indicates an increase in partition coefficients upon increasing the IL:NaSCN molar ratio from 1:1 to 1:2, while red shading denotes a decrease.

† Value not reported for MV due to phase-preference inversion between the two systems (IL:NaSCN = 1:1 and 1:2), which prevents a meaningful definition of relative change.

The most favorable balance between cost reduction and partition enhancement was observed for ammonium-based ILs. In particular, $[N_{2222}]$ and $[N_{3333}]$ systems exhibited substantial increases in the partition of the ferro/ferricyanide redox couple upon increasing NaSCN content, while achieving the same ~22% reduction in formulation cost. These results demonstrate that, for appropriately selected IL families, NaSCN substitution not only lowers cost but can also improve electrolyte separation, directly supporting the functional requirements of membrane-free redox flow batteries.

In membrane-free redox flow batteries, electrolyte cost represents a significant fraction of total system cost, while extensive partitioning is essential to avoid self-discharge and capacity fade. Strategies that simultaneously reduce electrolyte cost and maintain or enhance partition directly contribute to lowering capital expenditure and improving system viability, particularly in early-stage deployment scenarios where cost sensitivity is high. As discussed in recent analyses of membrane-free RFB commercialization, simplified and cost-efficient electrolyte formulations are critical for pilot-scale systems and behind-the-meter applications, which typically represent the first market entry points for emerging flow battery technologies [17].

4 Conclusion

The present work demonstrates that sodium thiocyanate enables liquid-liquid phase separation in chloride-based ionic liquid aqueous systems that otherwise form solid-liquid equilibria with conventional salting-out agents, expanding the accessible electrolyte design space for membrane-free configurations. Phase diagrams and partition coefficients were established to support electrolyte formulation and redox-molecule screening for membrane-free redox flow batteries.

Across the phase-separated systems, viologen and TEMPO derivatives preferentially partition to the top (IL-rich) phase, whereas ferrocyanide ($K_4[Fe(CN)_6]$) preferentially partitions into the bottom (salt-rich) phase, while ferricyanide ($K_3[Fe(CN)_6]$) shows this behavior only in systems based on $[N_{3333}]Cl$. The impact of NaSCN content on partitioning was formulation-dependent: increasing NaSCN from IL:NaSCN = 1:1 to 1:2 enhanced partitioning for selected combinations, most notably for the inorganic couple in ammonium-based systems, while decreasing partitioning in more hydrophilic systems such as those based on [C_2mim]Cl. In addition, MV exhibited a phase-preference inversion in at least one system. These results indicate that performance gains from NaSCN cannot be assumed a priori and must be evaluated at the composition level.

From an economic standpoint, partial replacement of the ionic liquid by NaSCN reduced the estimated material cost of the total ABS formulation by 21-24% for the studied compositions. In the best-performing cases, particularly ammonium-based systems, this cost reduction was achieved without negatively affecting the partitioning of the target redox couples. Overall, NaSCN is a practical formulation lever to enable phase separation in chloride-based ionic-liquid systems while offering a measurable cost advantage and, in selected systems, improved separation of relevant redox couples.

Future work should focus on expanding the chemical space toward more hydrophobic ionic liquids to enhance phase differentiation and enable a broader range of compatible redox couples. In addition, systematic optimization of electrolyte composition will be essential to maximize selectivity while maintaining favorable physicochemical properties. Finally, electrochemical validation of the most promising systems identified here will be critical to confirm their performance in membrane-free redox flow battery configurations.

CRediT Author Statement

Gabriel Camilo: Investigation, Validation, Data curation, Writing - Original Draft. **Murilo Leite Alcantara:** Conceptualization, Investigation, Formal analysis, Writing - Review & Editing, supervision, Project administration. **Ana M. Ferreira**: Methodology, Formal analysis, Writing - Review & Editing, Supervision. **Marco Prazeres**: Data curation, Writing - Review & Editing. **Catarina M.S.S. Neves**: Validation, Writing - Review & Editing, Supervision. **João A. P. Coutinho**: Conceptualization, Resources, Writing - Review & Editing, supervision, Project administration.

Declaration of competing interest

The authors declare that they have no known competing financial interests or personal relationships that could have appeared to influence the work reported in this paper.

Acknowledgments

This work was developed within the scope of the project CICECO Aveiro Institute of Materials, UID/50011/2025 (DOI 10.54499/UID/50011/2025) & LA/P/0006/2020 (DOI 10.54499/LA/P/0006/2020) , financed by national funds through the FCT/MCTES (PIDDAC). The authors acknowledge the financial support by the MeBattery project that has received funding from the European Innovation Council of the European Union under Grant Agreement no. 101046742. GLC acknowledge FCT for the Ph.D. grant UI/BD/00343/2024. AMF acknowledges FCT for the research contract CEECIND/00361/2022 (DOI 10.54499/2022.00361.CEECIND/CP1720/CT0020).

Declaration of generative AI and AI-assisted technologies in the writing process

During the preparation of this work, the authors used ChatGPT to improve readability and correct grammar and typographical errors. After using this tool, the authors reviewed and edited the content as needed and take full responsibility for the content of the publication.

Reference

[1] S. Mao, J. Chen, M. Liu, A review of the energy storage system as a part of power system: Modelling, simulation and prospect, Electr. Power Syst. Res. 233 (2024) 110448. https://doi.org/10.1016/J.EPSR.2024.110448.

[2] D.A. Elalfy, E. Gouda, M.F. Kotb, V. Bureš, B.E. Sedhom, Comprehensive review of energy storage systems technologies, objectives, challenges, and future trends,

Energy Strateg. Rev. 54 (2024) 110448. https://doi.org/10.1016/j.esr.2024.101482.

[3] C. Suresh, R.P. Saini, Thermal performance of sensible and latent heat thermal energy storage systems, Int. J. Energy Res. 44 (2020) 4743–4758. https://doi.org/10.1002/er.5255.

[4] L. Kalapala, J.K. Devanuri, Influence of operational and design parameters on the performance of a PCM based heat exchanger for thermal energy storage – A review, J. Energy Storage 20 (2018) 497–519. https://doi.org/10.1016/j.est.2018.10.024.

[5] K. Lourenssen, J. Williams, F. Ahmadpour, R. Clemmer, S. Tasnim, Vanadium redox flow batteries: A comprehensive review, J. Energy Storage 25 (2019) 100844. https://doi.org/10.1016/J.EST.2019.100844.

[6] S.H. Khan, Energy storage systems for deep decarbonization: A critical review, J. Energy Storage 150 (2026). https://doi.org/10.1016/j.est.2026.120485.

[7] M. Pan, M. Shao, Z. Jin, Development of organic redox-active materials in aqueous flow batteries: Current strategies and future perspectives, SmartMat 4 (2023). https://doi.org/10.1002/smm2.1198.

[8] I. Iwakiri, T. Antunes, H. Almeida, J.P. Sousa, R.B. Figueira, A. Mendes, Redox flow batteries: Materials, design and prospects, Energies (Basel). 14 (2021) 5643. https://doi.org/10.3390/en14185643.

[9] S. Ebner, S. Spirk, T. Stern, C. Mair-Bauernfeind, How Green are Redox Flow Batteries?, ChemSusChem 16 (2023) e202201818. https://doi.org/10.1002/cssc.202201818.

[10] X. Wang, R.K. Gautam, J. Jimmy Jiang, Recent advancements in membrane-free redox flow batteries, Chem. Soc. Rev. 54 (2025) 5895–5911. https://doi.org/10.1039/d5cs00174a.

[11] F.R. Brushett, M.J. Aziz, K.E. Rodby, On Lifetime and Cost of Redox-Active Organics for Aqueous Flow Batteries, ACS Energy Lett. 5 (2020) 879–884. https://doi.org/10.1021/acsenergylett.0c00140.

[12] J. Luo, B. Hu, M. Hu, Y. Zhao, T. Leo Liu, Status and Prospects of Organic Redox Flow Batteries toward Sustainable Energy Storage, ACS Energy Lett. 4 (2019) 2220–2240. https://doi.org/10.1021/acsenergylett.9b01332.

[13] M.O. Bamgbopa, Y. Shao-Horn, R. Hashaikeh, S. Almheiri, Cyclable membraneless redox flow batteries based on immiscible liquid electrolytes: Demonstration with all-iron redox chemistry, Electrochim. Acta 267 (2018) 41–50. https://doi.org/10.1016/J.ELECTACTA.2018.02.063.

[14] P. Navalpotro, C.M.S.S. Neves, J. Palma, M.G. Freire, J.A.P. Coutinho, R. Marcilla, Pioneering Use of Ionic Liquid-Based Aqueous Biphasic Systems as Membrane-Free Batteries, Adv. Sci. 5 (2018) 1800576. https://doi.org/10.1002/advs.201800576.

[15] E. Sánchez-Díez, E. Ventosa, M. Guarnieri, A. Trovò, C. Flox, R. Marcilla, F. Soavi, P. Mazur, E. Aranzabe, R. Ferret, Redox flow batteries: Status and perspective towards sustainable stationary energy storage, J. Power Sources 481 (2021) 228804. https://doi.org/10.1016/J.JPOWSOUR.2020.228804.

[16] A.F. Molina-Osorio, A. Gamero-Quijano, P. Peljo, M.D. Scanlon, Membraneless energy conversion and storage using immiscible electrolyte solutions, Curr. Opin. Electrochem. 21 (2020) 100–108. https://doi.org/10.1016/J.COELEC.2020.01.013.

[17] P. Navalpotro, J. Palma, V. Muñoz-Perales, A. Martínez-Bejarano, M.V. Martín-Arroyo, D.P. Taylor, A. Platek-Mielczarek, P.G. Rivano, F. Paratore, E.D. Re, R. Marcilla, Membrane-free redox flow battery: From the idea to the market, APE 3 (2025) 012001. https://doi.org/10.1063/5.0231462.

[18] J. Liu, J. Deng, Y. Hua, C. Liu, X. Zhang, M. Li, Y. Shao, A Triphasic Membrane-Free Redox Flow Battery in a Total Aqueous System, ACS Appl. Energy Mater. 7 (2024) 12131–12140. https://doi.org/10.1021/acsaem.4c02805.

[19] P. Navalpotro, J. Palma, M. Anderson, R. Marcilla, A Membrane-Free Redox Flow Battery with Two Immiscible Redox Electrolytes, Angew. Chem. Int. Ed. 56 (2017) 12460–12465. https://doi.org/10.1002/anie.201704318.

[20] P. Peljo, M. Bichon, H.H. Girault, Ion transfer battery: Storing energy by transferring ions across liquid-liquid interfaces, Chem. Commun. 52 (2016) 9761–9764. https://doi.org/10.1039/c6cc04325a.

[21] G.L. Soloveichik, Flow Batteries: Current Status and Trends, Chem. Rev. 115 (2015) 11533–11558. https://doi.org/10.1021/cr500720t.

[22] Y. Shu, H. Xiao, Y. Yu, Z. Yu, Y. Lin, Y. Sun, J. Huang, Toward Membrane-Free Flow Batteries, ACS Appl. Energy Mater. 8 (2025) 8710–8725. https://doi.org/10.1021/acsaem.5c00799.

[23] I.M. Gutierrez, R. Marcilla, J. García, P. Del Val, E. Ventosa, Arbaizar Marcos, V. Coello, M. Sanchez Anz, Santiago Enrique, L. Ibanez, Redox flow battery with immiscible electrolyte and flow through electrode, EP4136694A1, 2021.

[24] M.L. Alcantara, P. Navalpotro, G. Camilo, M. Prazeres, C.M.S.S. Neves, A.M. Ferreira, E. Ventosa, R. Marcilla, J.A.P. Coutinho, Tuning biphasic electrolytes for membrane-free redox flow batteries: influence of sodium thiocyanate on partition and viscosity, J. Mol. Liq. 439 (2025) 128767. https://doi.org/10.1016/J.MOLLIQ.2025.128767.

[25] L. Nie, Z. Zheng, M. Lu, S. Yao, D. Guo, Phase Behavior of Ionic Liquid-Based Aqueous Two-Phase Systems, Int. J. Mol. Sci. 23 (2022) 12706. https://doi.org/10.3390/ijms232012706.

[26] T. Hamamoto, M. Okai, S. Katsuta, The Laws Governing Ionic Liquid Extraction of Cations: Partition of 1-Ethylpyridinium Monocation and Paraquat Dication in Ionic Liquid/Water Biphasic Systems, J. Phys. Chem. B 119 (2015) 6317–6325. https://doi.org/10.1021/acs.jpcb.5b02923.

[27] S. Shahriari, C.M.S.S. Neves, M.G. Freire, J.A.P. Coutinho, Role of the Hofmeister Series in the Formation of Ionic-Liquid-Based Aqueous Biphasic Systems, J. Phys. Chem. B 116 (2012) 7252–7258. https://doi.org/10.1021/jp300874u.

[28] P. Phogat, S. Dey, M. Wan, Comprehensive review of Sodium-Ion Batteries: Principles, Materials, Performance, Challenges, and future Perspectives, Mater. Sci. Eng. B. 312 (2025) 117870. https://doi.org/10.1016/J.MSEB.2024.117870.

[29] V. Palomares, P. Serras, I. Villaluenga, K.B. Hueso, J. Carretero-González, T. Rojo, Na-ion batteries, recent advances and present challenges to become low cost

energy storage systems, Energy Environ. Sci. 5 (2012) 5884–5901. https://doi.org/10.1039/c2ee02781j.

[30] Y. Zhang, P.S. Cremer, Interactions between macromolecules and ions: the Hofmeister series, Curr. Opin. Chem. Biol. 10 (2006) 658–663. https://doi.org/10.1016/j.cbpa.2006.09.020.

[31] T. Liu, X. Wei, Z. Nie, V. Sprenkle, W. Wang, A Total Organic Aqueous Redox Flow Battery Employing a Low Cost and Sustainable Methyl Viologen Anolyte and 4-HO-TEMPO Catholyte, Adv. Energy Mater. 6 (2016) 1501449. https://doi.org/10.1002/aenm.201501449.

[32] V. Singh, S. Kim, J. Kang, H.R. Byon, Aqueous organic redox flow batteries, Nano Res. 12 (2019) 1988–2001. https://doi.org/10.1007/s12274-019-2355-2.

[33] A. Ramar, F.M. Wang, R. Foeng, R. Hsing, Organic redox flow battery: Are organic redox materials suited to aqueous solvents or organic solvents?, J. Power Sources 558 (2023) 232611. https://doi.org/10.1016/j.jpowsour.2022.232611.

[34] C.M.S.S. Neves, S.P.M. Ventura, M.G. Freire, I.M. Marrucho, J.A.P. Coutinho, Evaluation of Cation Influence on the Formation and Extraction Capability of Ionic-Liquid-Based Aqueous Biphasic Systems, J. Phys. Chem. B 113 (2009) 5194–5199. https://doi.org/10.1021/jp900293v.

[35] V. Najdanovic-Visak, J.N. Canongia Lopes, Z.P. Visak, J. Trindade, L.P.N. Rebelo, Salting-out in aqueous solutions of ionic liquids and K 3PO 4: Aqueous biphasic systems and salt precipitation, Int. J. Mol. Sci. 8 (2007) 736–748. https://doi.org/10.3390/i8080736.

[36] H. Passos, T.B. V Dinis, E. V Capela, M. V Quental, J. Gomes, J. Resende, P.P. Madeira, M.G. Freire, J.A.P. Coutinho, Mechanisms ruling the partition of solutes in ionic-liquid-based aqueous biphasic systems – the multiple effects of ionic liquids, Phys. Chem. Chem. Phys. 20 (2018) 8411–8422. https://doi.org/10.1039/C8CP00383A.

[37] Y. Marcus, Thermodynamics of solvation of ions. Part 5. - Gibbs free energy of hydration at 298.15 K, J. Chem. Soc., Faraday Trans. 87 (1991) 2995–2999. https://doi.org/10.1039/FT9918702995.

[38] N. V. Plechkova, K.R. Seddon, Applications of ionic liquids in the chemical industry, Chem. Soc. Rev. 37 (2008) 123–150. https://doi.org/10.1039/b006677j.

Declaration of interests

☒ The authors declare that they have no known competing financial interests or personal relationships that could have appeared to influence the work reported in this paper.

☐ The authors declare the following financial interests/personal relationships which may be considered as potential competing interests: